

Published in final edited form as:

*Cancer Res.* 2018 October 15; 78(20): 5863–5876. doi:10.1158/0008-5472.CAN-18-0855.

## PTTG and PBF functionally interact with p53 and predict overall survival in head and neck cancer

Martin L Read<sup>#1,\*</sup>, Bhavika Modasia<sup>#1</sup>, Alice Fletcher<sup>1</sup>, Rebecca J. Thompson<sup>1</sup>, Katie Brookes<sup>1</sup>, Peter C Rae<sup>2</sup>, Hannah R Nieto<sup>1</sup>, Vikki L Poole<sup>1</sup>, Sally Roberts<sup>2</sup>, Moray J Campbell<sup>3</sup>, Kristien Boelaert<sup>1</sup>, Andrew S Turnell<sup>2</sup>, Vicki E Smith<sup>1</sup>, Hisham Mehanna<sup>2</sup>, and Christopher J McCabe<sup>1,\*</sup>

<sup>1</sup>Institute of Metabolism and Systems Research, University of Birmingham, Birmingham, B15 2TH, UK

<sup>2</sup>Institute of Cancer and Genomic Sciences, University of Birmingham, Birmingham, B15 2TT, UK

<sup>3</sup>Division of Pharmaceutics and Pharmaceutical Chemistry, College of Pharmacy, The Ohio State University, Columbus, OH, 43210, USA

# These authors contributed equally to this work.

### Abstract

Head and neck squamous cell carcinoma (HNSCC) is the 6th most common cancer worldwide and poses a significant health burden due to its rising incidence. Although the proto-oncogene pituitary tumor transforming gene 1 (PTTG) predicts poor patient outcome, its mechanisms of action are incompletely understood. We show here that the protein PBF modulates PTTG function, is overexpressed in HNSCC tumors, and correlates with significantly reduced survival. Lentiviral shRNA attenuation of PTTG or PBF expression in HNSCC cells with either wild type or mutant p53, and with and without HPV infection, led to dysregulated expression of p53 target genes involved in DNA repair and apoptosis. Mechanistically, PTTG and PBF affected each other's interaction with p53 and cooperated to reduce p53 protein stability in HNSCC cells independently of HPV. Depletion of either PTTG or PBF significantly repressed cellular migration and invasion and impaired colony formation in HNSCC cells, implicating both proto-oncogenes in basic mechanisms of tumorigenesis. HNSCC patients with high tumoral PBF and PTTG had the poorest overall survival, which reflects a marked impairment of p53-dependent signalling.

### Keywords

PTTG; PBF; HNSCC; PTTG1IP; p53

---

\*Corresponding authors: Martin L Read and Christopher J McCabe, Institute of Metabolism and Systems Research, College of Medical and Dental Sciences, University of Birmingham, Birmingham, B15 2TH, UK. Phone: 44 121 415 8713; Fax: 44 121 415 8712; m.l.read.20@bham.ac.uk; mccabcjz@bham.ac.uk.

Conflict of interest: The authors assert they have no conflicts of interest.

## Introduction

Worldwide, more than 687,000 new cases of head and neck cancer were diagnosed in 2015 and 380,000 deaths (1, 2). HNSCC is a heterogeneous group of malignancies, displaying vastly different biological and clinical features (3–6). Several main classes of risk factor have been identified, including tobacco and alcohol consumption, and HPV infection. Most tumours demonstrate copy number alterations and high levels of genetic instability (7). Concordantly, TP53 mutations have historically been reported in ~50-80% of HNSCC cases (8, 9), whilst The Cancer Genome Atlas (TCGA) recently reported p53 mutations among HPV-ve samples at a higher rate of 86% (7). Loss of p53 function through its interaction with the HPV E6 oncoprotein or loss of heterozygosity (LOH) is thought to occur in an additional ~20% of HNSCC tumours (8–10). In remaining tumours harbouring wild-type TP53, disruption of the p53 pathway may be elicited via the specific targeting of p53-related proteins.

Multiple proteins are known to regulate p53 function. Separately, the proto-oncogenes pituitary tumor transforming gene 1 (PTTG) and its interacting partner PBF have been shown to bind p53 in various cellular models (11–13). As such, PTTG and PBF represent an interesting paradigm of p53 regulation: two proto-oncogenes which are independently upregulated in several tumour types, inherently multifunctional, implicated in poor prognosis, and whose essential mechanisms of action have not yet been fully delineated.

Several studies have independently demonstrated overexpression of PTTG in oesophageal squamous cell carcinoma (ESCC) (14–18). Indeed, high tumoural PTTG expression has been found to strongly correlate with advanced pathological stage, extensive lymph node metastasis and reduced survival (16–18), indicating that PTTG may serve as a novel prognostic marker for ESCC (14, 19). PBF, however, has not been examined in the context of head and neck cancer. Previous studies demonstrated that a functional interaction exists between PBF and p53 in thyroid and colorectal cancer (12, 13, 20). PBF was shown to significantly reduce p53 stability via induction of MDM2-mediated ubiquitination and proteasomal degradation (12). Furthermore, PBF significantly repressed p53-mediated transactivation of genes and was associated with increased genomic instability (12, 13).

Whilst TP53 mutation is common in HNSCC, p53 mutations occur in fewer than 1% of differentiated thyroid cancers (DTC) (21). We recently demonstrated that thyroid-specific bi-transgenic mice (Bi-Tg) showed significant perturbations in p53 pathway genes (20), indirectly suggesting that inactivation of p53 – rather than mutation – may be an aetiological event in DTC. In HNSCC, p53 inactivation may be achieved by several mechanisms, such as expression of HPV E6 and overexpression/amplification of HDM2 (10). Given that PTTG has been reported to be upregulated in HNSCC tumours, and PBF in multiple tumour types (13, 22, 23), we hypothesised that the interacting partners PTTG and PBF are both overexpressed in HNSCC and high tumoural levels are associated with poor prognosis. We further hypothesised that PTTG and PBF bind p53 in the setting of head and neck cancer, and hence inactivate its tumour suppressor function, which may serve to promote tumorigenesis and progression.

Our data reveal a complex inter-relationship between PTTG, PBF and p53 expression and function *in vitro* and *in vivo*. We show that PBF is overexpressed in HNSCC tumours, and correlates with poorer clinical outcome. Depletion of PTTG and PBF in HNSCC cells significantly attenuated cell migration and invasion, and resulted in dysregulated p53 signalling. We propose a novel model by which PTTG and PBF interact in HNSCC to reduce p53 stability and hence function.

## Materials and Methods

### Human tissue samples

Matched tumour and normal tissue specimens were obtained from 24 patients undergoing surgery for HNSCC at the University Hospital Birmingham NHS Trust, UK (Supplementary Table S1). Tissue microarrays (TMA) were prepared with HNSCC tissue from 53 patients undergoing surgery at multiple hospital sites (Supplementary Table S2). Specimens at the time of surgery were obtained in accordance with the World Medical Association (WMA) Declaration of Helsinki ethical guidelines and written informed consent from patients. Ethical approval was granted by the Yorkshire and the Humber-Leeds East National Research Ethics Service (NRES) committee (REC no. 14/YH/1101, secondary objective 10). All studies were approved by an institutional review board.

### Cell culture

HNSCC (92-VU-040T, 93-VU-147T) cell lines were kindly provided by Prof Hans Joenje (VU University Medical Center, Amsterdam, the Netherlands), and HeLa cells were obtained from ECACC. All cells were maintained in DMEM (Sigma-Aldrich) supplemented with 10% fetal bovine serum, penicillin ( $10^5$  U/l), and streptomycin (100 mg/l). Cells were cultured at low passage and authenticated by short tandem repeat analysis (NorthGene, Newcastle upon Tyne, UK) (Supplementary Fig. S1A and S1B) and tested for mycoplasma contamination (EZ-PCR kit; Geneflow). HNSCC cells stably transduced with PTTG, PBF or Scrambled (Scr) shRNA were generated using the BLOCK-iT lentiviral RNAi expression system (Invitrogen) or pre-designed, transduction-ready SMARTvector 2.0 lentiviral particles expressing specific shRNA sequences (Dharmacon) as per manufacturer's instructions. Further information on HNSCC cells and shRNA sequences are provided (Supplementary Tables S3 and S4).

### Western blotting and Immunohistochemistry

Western blot and p53 stability assays were performed as described previously (12, 23, 24). Primary antibodies used are listed in Supplementary Table S5. Formalin fixed paraffin embedded tissue sections were immunostained using the Novocastra™ Novolink™ Max Polymer Detection system (Leica Biosystems) as per manufacturer's instructions. DNA damage was induced by Caesium-137 irradiation using an irradiator IBL 437C type H unit (CIS Bio international). Protein and RNA were harvested at 24h post-irradiation.

### Co-immunoprecipitation

Cells were harvested in modified RIPA buffer (150 mM sodium chloride, 50 mM Tris pH 7.4, 6 mM sodium deoxycholate, 1 % v/v Igepal CA-630 and 1 mM ethylene glycol

tetraacetic acid (EGTA)) containing 60 µl/ml of Protease Inhibitor Cocktail (104 mM 4-(2-aminoethyl)benzenesulfonyl fluoride (AEBSF), 80 µM Aprotinin, 4 mM Bestatin, 1.4 mM E-64, 2 mM Leupeptin and 1.5 mM Pepstatin A in dimethyl sulfoxide (DMSO)) [Sigma-Aldrich]. Samples were sonicated twice for 30 s (medium setting; Diagenode Bioruptor® - Diagenode, Seraing, Belgium) before microcentrifugation at 4°C for 30 min. Cell lysates were transferred to a clean microcentrifuge tube and 50 µl removed and stored at -20°C.

Primary antibody was then added to the remaining cell lysate and incubated overnight at 4°C with end-over-end mixing. Protein G sepharose beads [GE Healthcare Life Sciences, Little Chalfont, Buckinghamshire, UK] were pulse centrifuged and resuspended in modified RIPA buffer. 50 µl of protein G sepharose bead slurry was then added and samples incubated at 4°C with end-over-end mixing for a further 2 h. Samples were pulse centrifuged to pellet beads and supernatant discarded. Unbound protein was eliminated by washing beads in modified RIPA buffer followed by pulse centrifugation. Bound protein was eluted in 2x loading buffer (1:20 β-mercaptoethanol and 1% SDS in Laemmli buffer [Bio-rad Laboratories Ltd, Hemel Hempstead, Hertfordshire, UK]) and incubated at 37°C for 30 min. Loading buffer was added at 1:1 ratio (v:v) to IP samples and whole cell lysates prior to Western blotting. No antibody (Nab) and an IgG isotype antibody (ISO) were used as negative controls.

### Cell movement and proliferation

2D Boyden chamber invasion assays were performed according to manufacturer's instructions. Classical scratch wound healing assays were performed using standard protocols and live cell images taken with a Nikon Inverted Confocal/TIRF microscope. BrdU ELISA kit (Roche) was used to assess proliferation as per manufacturer's instructions.

### Nucleic acids and transfection

Plasmids containing PBF, PTTG, PBF M1 and PTTG BD- cDNA have been described elsewhere (22, 24). Transfections were performed with TransIT-LT1 (GeneFlow) using standard protocols. Total RNA was extracted using the RNeasy Micro Kit (Qiagen) prior to reverse transcription using the Reverse Transcription System (Promega). Expression of specific mRNAs was determined on a 7500 Real-time PCR system (Applied Biosystems) using primers listed in Supplementary Table S6.

### TCGA data analysis

Normalized gene expression data generated using the Illumina RNA-seq platform and clinical information were downloaded from cBioPortal (25, 26) and FireBrowse (27). Gene expression values were transformed as  $X = \log_2(X+1)$  where X represents the normalized fragments per kilobase transcript per million mapped reads (FPKM) values. For matched normal (N) and tumour (C) pairs, relative fold-changes (FC) were transformed as  $\log_2 FC = \log_2(C) - \log_2(N)$ , where C and N represent normalised FPKM values. In total RNAseq data for 520 unmatched HNSCC samples were analysed, including 72 HPV-ve, 39 HPV+ve, 157 wild-type p53 and 363 mutant p53 tumour specimens. From these, survival data was available for 517 HNSCC patients including those with wild-type p53 ( $n = 157$ ) and mutant

( $n = 360$ ) p53 tumours. 43 matched tumour and normal samples in HNSCC TCGA were also analysed.

### Survival analysis

Kaplan-Meier analysis was used to estimate overall (OS) and disease-free (DFS) survival. Median survival (OS and DFS) was estimated at the smallest time at which the survival probability dropped to 0.5 or below. Tests were used to compare the equality of survival distributions as follows: (i) Log rank ( $P_L$ ). All time points are weighted equally which emphasizes longer survival times, (ii) Breslow ( $P_B$ ). Time points are weighted by the number of cases at risk at each time point which emphasizes shorter survival times, and (iii) Tarone-Ware ( $P_T$ ). Time points are weighted by the square root of the number of cases at risk at each time point which emphasizes intermediate survival times.

### Cut off determination for patient stratification

The median value of PBF and PTTG expression ( $\log_2$ ) in either wild-type ( $n = 157$ ) or mutant p53 ( $n = 360$ ) tumours was used as a cut off to stratify HNSCC patients with either high or low joint PBF/PTTG expression in lymph node and survival analysis. This approach enabled the maximum number of patients with high or low tumoural PBF/PTTG to be stratified.

### Statistical analysis

All results were obtained from triplicate independent experiments unless otherwise indicated. Non-parametric Kolmogorov-Smirnov, Kruskal-Wallis, Mann-Whitney and Spearman's correlation tests were performed as expression levels were not normally distributed in TCGA. Normal distribution was tested using the D'Agostino-Pearson test of normality. Data were analysed using IBM SPSS Statistics (version 22) and Microsoft Excel.  $P < 0.05$  were considered significant.

## Results

### Elevated PTTG expression and phosphorylation

To examine PTTG expression we initially assessed mRNA levels in matched tumour and normal tissue from HNSCC patients and found significant upregulation (1.9-fold,  $n=24$ ; Fig. 1A and B; Supplementary Table S1). This was consistent with TCGA RNA-seq data which revealed significant elevation in tumoural PTTG mRNA in matched ( $n=43$ ; Fig. 1C) and unmatched samples ( $n=520$ ; Supplementary Fig. S2A). In particular, PTTG expression was greater in HPV+ve tumours ( $P=2.76 \times 10^{-11}$ ;  $n=39$ ; Fig. 1D), as well as being increased in HNSCC irrespective of p53 status whether they were wild-type (WT) ( $P=2.96 \times 10^{-13}$ ;  $n=157$ ) or mutant p53 (MUT p53) ( $P=9.38 \times 10^{-9}$ ;  $n=363$ ; Fig. 1E) compared to normals. Apart from the hypopharynx, PTTG expression in oropharyngeal tumours was significantly higher than at other subsites (Supplementary Fig. S2B) which coincided with a greater incidence of WT p53 and HPV+ve HNSCC (Supplementary Fig. S2C-S2E; Supplementary Table S7). PTTG was also abundantly expressed in HNSCC cell lines (Fig. 1F).

Given the recent discovery that PTTG has a phosphorylatable T60 residue which alters protein half-life, as well as influencing genetic instability and cell invasion (28), we next examined total PTTG and PTTG-pT60 protein using TMA specimens (Supplementary Table S2). To do this, we generated a PTTG-pT60 antibody and demonstrated for the first time that PTTG is phosphorylated at residue T60 *in vivo* (Fig. 1G). In particular, total and T60-phosphorylated PTTG protein were predominantly nuclear in localisation, and abundantly expressed in tumours (Fig. 1G; Supplementary Fig. S3). In keeping with TCGA, HPV+ve tumours had significantly higher total PTTG than HPV-ve tumours (Supplementary Table S8). We validated the PTTG-pT60 antibody by identifying a specific product at ~30 kDa in WT PTTG-transfected HeLa cells (Fig. 1H), which was significantly reduced with mutant T60A and VO control (Fig. 1H and I). Preincubation of the PTTG-pT60 antibody with a neutralising peptide ablated detection of pT60 PTTG protein (Fig. 1J and K), whilst PTTG knockdown abolished total and pT60 PTTG protein expression (Fig. 1L).

### **PBF expression correlates with poorer survival**

PBF has not been investigated in HNSCC before. In our matched specimens, PBF mRNA expression was significantly higher in tumour tissue than in normal (1.6-fold,  $n=24$ ; Fig. 2A and B). PBF and PTTG mRNA expression correlated (Fig. 2C), suggesting, as before in the thyroid (22), a common pathway of regulation. In keeping with our in-house findings, tumoural PBF expression was also significantly increased in matched ( $n=43$ ; Fig. 2D) and unmatched ( $n=363$ ; Fig. 2E; Supplementary Fig. S4A) TCGA samples compared to normals. In contrast to PTTG, PBF expression was not influenced by HPV status (Fig. 2F) and there was no significant difference in expression between tumour subsites (Supplementary Fig. S4A). Of particular significance, patients with higher tumoural PBF expression had significantly reduced survival in the unmatched TCGA dataset especially at earlier time points (Fig. 2G; Supplementary Fig. S4B). Similar to PTTG, PBF was highly expressed in HNSCC cell lines (Supplementary Fig. S4C).

In accordance with these findings, total PBF protein was highly abundant in our TMA series which appeared to be both nuclear and cytoplasmic, similar to that seen in thyroid and breast cancer (22, 23) (Fig. 2H). Phosphorylation at residue Y174 is critical in modulating PBF activity in oncogenic processes (29, 30). Here, we also observed strong immunostaining of PBF-pY174 in oropharyngeal tumours of all tumour grades (Fig. 2H; Supplementary Fig. S4D). By comparison, normal tissue displayed only weak to moderate expression of total PBF and PBF-pY174 (Fig. 2H).

### **PTTG and PBF modulate migratory and invasive properties of HNSCC cells**

Overexpression of PTTG and PBF is associated with increased tumour invasiveness and cell migration in multiple settings (13, 17, 30–32). To gain insights into the role of PTTG and PBF in HNSCC, we generated four lentiviral shRNA knockdown lines of PTTG and PBF using 92-VU-040T and 93-VU-147T cells, and achieved greater than 80% protein and mRNA knockdown (Fig. 3A and B). Subsequent scratch-wound cell migration assays demonstrated that PTTG ablation markedly reduced the rate of wound closing in 92-VU-040T ( $54.5\pm 5.5\%$  vs.  $22.5\pm 3.7\%$  at 8h; Fig. 3C) and 93-VU-147T ( $70.0\pm 3.6\%$  vs.  $49.5\pm 3.6\%$  at 24h; Supplementary Fig. S5A) cells compared to controls. Similarly, shRNA



knockdown of PBF resulted in a significant reduction in the number of migrating HNSCC cells (Fig. 3D; Supplementary Fig. S5B).

The impact of PTTG and PBF depletion on cell invasion was also robust. Our results in 2D Boyden chamber invasion assays, for instance, showed greater than 80% inhibition of the inherent invasive capacity of both PTTG-knockout HNSCC cell lines (Fig. 3E), with similar data following PBF ablation (Fig. 3F). A marked decrease in colony formation was also evident in PTTG- and PBF-depleted cells (Supplementary Fig. S5C and S5D).

Overall these results indicate that HNSCC cells require PTTG and PBF for effective cell migration and invasion *in vitro*, implicating both genes in fundamental mechanisms of cell movement. This does not appear to be an indirect effect of altered cell proliferation given the relatively modest effects of PTTG and PBF ablation on cell turnover (Fig. 3G).

### Correlation of PTTG and PBF with p53-target genes and patient survival

PTTG and PBF have been implicated in central mechanisms of DNA repair, apoptosis and cell cycle regulation (12, 20, 33–35), involving both p53-dependent and p53-independent pathways. Having identified a critical role for PTTG and PBF in HNSCC cell movement, we next investigated their relationship with p53-target genes. In TCGA there was a striking correlation with PTTG and a panel of 129 p53-target genes (20) in WT p53 HNSCC (82% genes; Fig 4A; Supplementary Fig. S6A and S6B). The correlation signature of PTTG and p53-target genes was shifted between WT and MUT p53 HNSCC (Fig. 4A and B). Considerable differences in MUT p53 HNSCC were apparent, for instance, with several p53-target genes such as BCL2 (Fig. 4C; mean  $\rho=0.233\pm 0.01$ ), which was associated with a significant change in gene expression (Supplementary Fig. S6C and S6D). A large proportion of p53-target genes were however still correlated significantly with PTTG in MUT p53 HNSCC (68% genes; Supplementary Fig. S7A-S7C), which was also evident in TCGA cohorts of matched size (Fig. 4D).

By comparison, PBF expression correlated with fewer p53-target genes in HNSCC (WT p53: 18% genes; MUT p53: 38% genes; Supplementary Fig. S8A-S8C). Importantly, p53-target genes showed a significantly more negative correlation with PBF expression than the background transcriptome, supporting a functional relationship (WT p53:  $P=0.0006$ ; MUT p53:  $P=9.0\times 10^{-6}$ ; Supplementary Fig. S8D). Several p53-target genes identified such as Ube2a and XRCC3 (Supplementary Fig. S8E and S8F) have been previously associated with PBF in thyroid cancer (12). In contrast to PTTG, PBF expression correlated with a similar or slightly greater number of p53-target genes in MUT p53 HNSCC cohorts of matched size (Fig. 4D).

In agreement with this, there were significant mRNA changes in our PTTG- and PBF-depleted HNSCC cells for p53-responsive genes such as BCL2, RAD51 and BRCA1 (Fig. 4E and F). As PTTG and PBF have been implicated in modulating p53 responses following DNA damage (20), we next validated a robust p53 response in irradiated cells (Fig. 4G) and showed that removal of PTTG led to an enhanced response of BCL2 to  $\gamma$ -irradiation in both cell lines (Fig. 4H and I). PBF ablation did not alter BCL2 expression in irradiated cells but was associated with an enhanced CDKN1A response (Supplementary Fig. S8G and S8H).

Having observed significant correlation of PTTG and PBF with p53-target genes, we next evaluated whether this was associated with patient survival. Overall, HNSCC patients with p53 mutations in TCGA had poorer survival than those with WT p53 ( $P_L=0.00128$ ; Supplementary Fig. S9A; (36)). Of significance to our study, MUT p53 HNSCC patients with high tumoural PTTG had poorer overall survival ( $P_L=0.0032$ ; median OS=35.51 months) than those with low PTTG ( $P_L=NS$ ; median OS=52.27; Fig. 4J; Supplementary Table S9) compared to WT p53 HNSCC, as well as reduced disease-free survival (Supplementary Fig. S9B). Equally, overall survival was worse in MUT p53 HNSCC patients with high tumoural PBF (median OS=32.19 months; Fig. 4K; Supplementary Table S9).

Importantly, similar trends were observed in WT p53 HNSCC with a significant reduction in survival of patients with high tumoural PBF and PTTG expression (Supplementary Fig. S9C-S9E). In addition, HNSCC patients with HPV-ve tumours and high PTTG or PBF had poorer survival than those with low expression compared to HPV+ve HNSCC (Supplementary Fig. S9F and S9G). Altogether, these results show for the first time that high tumoural expression of PTTG and PBF are both associated with poorer survival characteristics in HNSCC, as well as dysregulated p53 responses in HNSCC cells.

### PTTG and PBF reciprocally alter the stringency of binding to p53

Independently, PTTG and PBF have both been shown to bind p53 *in vitro*, although controversy exists over the veracity and nature of PTTG:p53 binding (37). Given the relevance of correct p53 function to the aetiology of HNSCC, we investigated precisely how PTTG and PBF interact with p53.

Co-immunoprecipitation (co-IP) studies confirmed that PTTG and PBF specifically interact with endogenous p53 in HNSCC cells (Fig. 5A and B; Supplementary Fig. S10A). Reciprocal co-IPs further demonstrated successful interaction (Fig. 5C and D; Supplementary Fig. S10B-S10C). Thus, ‘forward’ and ‘reverse’ co-IPs demonstrate that PTTG and PBF are specific interactors of p53 in HNSCC cells. Next, we mapped the stringency of PTTG interaction with p53 in the presence and absence of PBF, and vice versa. PTTG retained the ability to bind p53 in the absence of PBF, but the degree of interaction was significantly attenuated (PBF-depleted 92-VU-040T cells:  $0.25\pm 0.06$ -fold and 93-VU-147T cells:  $0.67\pm 0.13$ -fold; Fig. 5E; Supplementary Fig. S10D). By contrast, PBF binding to p53 was markedly increased in the absence of PTTG (PTTG-depleted 92-VU-040T cells:  $4.0\pm 0.61$ -fold and 93-VU-147T cells:  $3.6\pm 0.25$ -fold; Fig. 5F; Supplementary Fig. S10E).

Based on these data, we hypothesise that PBF may facilitate PTTG binding to p53, whereas removal of PTTG enables more cellular PBF to interact with p53.

### PTTG and PBF alter the dynamics of p53 stability

To gain further insight into potential clinical relevance, we assessed joint overexpression of PBF and PTTG and found they were simultaneously upregulated in 37.2% of matched HNSCC tumour and normal samples (Fig. 5G;  $n=16/43$ ) compared to 88% of samples with either PBF or PTTG positive expression (Fig 5G;  $n=38/43$ ). We next investigated the



mechanistic consequences of PBF and PTTG binding to p53 by examining the intracellular stability of p53. Half-life studies using anisomycin to inhibit *de novo* protein synthesis showed that overexpression of PTTG resulted in a significant increase in p53 protein turnover in 92-VU-040T cells, with a ~5.5-fold reduction in p53 protein at 120 min ( $P=0.002$ ; Fig. 6A-C). Similarly, exogenous PBF significantly increased turnover of p53 protein in 92-VU-040T cells by ~6-fold ( $P=0.001$ ; Fig. 6A-C). Of particular significance, co-transfection of both PBF and PTTG resulted in the most pronounced reduction (~13-fold) in p53 protein stability at 120 min ( $P=0.0008$ ; Fig. 6A-C). A similar pattern of diminished p53 protein stability was seen in 93-VU-147T cells with high PBF+PTTG (~12-fold,  $P=0.005$ ; Supplementary Fig. S10F-S10H). By comparison, the reduction in p53 protein in VO control cells was modest at ~2-fold or lower at all time points (Fig. 6C; Supplementary Fig. S10H).

We then probed the interdependency of PTTG and PBF in modulating p53 stability through the use of the PTTG BD- mutant (cannot bind PBF) (22, 38) and PBF M1 mutant (cannot bind PTTG) (12). In contrast to HNSCC cells overexpressing PBF+PTTG, co-transfection of PBF M1+PTTG or PBF M1+PTTG BD- failed to significantly alter p53 protein stability compared to VO control cells at 120 min (Fig. 6D and E; Supplementary Fig. S10I-S10K). There was however a marked reduction in p53 protein stability with PBF and PTTG BD- in 92-VU-040T (~4-fold,  $P=0.004$ ; Fig. 6D; Supplementary Fig. S10I) and 93-VU-147T (~6-fold,  $P=0.005$ ; Supplementary Fig. S10I and S10K) cells compared to VO-controls, although the magnitude of p53 turnover was lower than with wild-type PBF+PTTG (Supplementary Fig. S10I).

These data demonstrate the importance of the specific interaction between PBF and PTTG in mediating a significant decrease in p53 stability. In particular, our findings suggest the following rules: (i) if PTTG cannot bind PBF, p53 stability is still repressed by PBF; (ii) if PBF cannot bind PTTG, PTTG loses the ability to decrease p53 stability; (iii) if neither PTTG nor PBF can interact, p53 stability is no longer repressed in HNSCC cells.

In support of this, we identified p53-target genes with unique transcriptional signatures in HNSCC with high PBF/PTTG compared to other expression subgroups (MUT p53: Fig. 6F and G; WT p53: Supplementary Figure S11A). Additionally, there was greater correlation of PBF expression with p53-target genes in WT p53 HNSCC with high PBF/PTTG (60/129 genes; Supplementary Fig. S11B), as well as more invasive metastatic disease (N1-N3;  $P=0.0002$ ; Fig. 6H; Supplementary Fig. S11C-S11E). Likewise in MUT p53 tumours with high PBF/PTTG, there was extensive correlation of PBF with p53-target genes (54/129 genes; Supplementary Fig. S12A), as well as poorer overall survival (median OS=28.98 months; Fig. 6I; Supplementary Fig. S12B), which associated with lower BCL2 expression and worse survival (Supplementary Fig. S12C-S12E). Finally, the genomic copy number loss of WT p53 in HNSCC (Supplementary Fig. S13A-S13E) disrupted the transcriptional relationship between PBF and PTTG with p53-target genes (Supplementary Fig. S14A-S14D).

Taken together, our study reveals multiple critical roles for PTTG and PBF in the pathogenesis of HNSCC which is associated with poor survival characteristics. In particular,

we propose that the ability of PBF to interact with PTTG results in greater impairment of p53-dependent signalling thereby contributing towards worse outcomes in HNSCC. A model of PTTG, PBF and p53 interaction in HNSCC is outlined (Fig. 7A-C).

## Discussion

Large-scale studies have provided considerable insights into genomic alterations associated with head and neck cancer (7, 39). Despite this, the mechanisms governing HNSCC tumorigenesis still remain to be fully defined due in part to a lack of understanding of proteins that interact and modify key effectors of oncogenesis. Our current study now identifies a significant functional interaction between PBF with PTTG and p53, which are both integral in the pathogenesis of HNSCC, thereby implicating PBF as an important aetiological factor in HNSCC.

High tumoural expression of PTTG has been independently correlated with advanced tumour stage, lymph node involvement and reduced disease-free survival (14, 16–18). In the present study, PTTG was abundant in HNSCC tissue with a significant correlation existing between PTTG and HPV status, which was confirmed by TCGA data. Similarly, T60-phosphorylated PTTG was overexpressed in HNSCC tumours, which has been implicated in genetic instability and cell invasion (28).

Importantly, this study now demonstrates for the first time that mRNA and protein expression of PTTG's interacting partner PBF were significantly increased in HNSCC tumours. A parallel increase in PBF and PTTG mRNA expression was evident in these samples. Given that PBF is required for the nuclear translocation of PTTG and for its transcriptional activity (38) and PBF mRNA expression is upregulated by PTTG in the thyroid (22), induction of PBF may be a secondary effect mediated by PTTG. Alternatively, correlated PBF and PTTG expression may be a result of a common regulatory mechanism; for example, oestrogen is known to regulate expression of both PBF and PTTG (23, 40, 41). One important facet of PBF expression was apparent in the larger public TCGA dataset: patients with high PBF mRNA expression had a lower survival than those with low expression. Whilst the mechanism remains to be fully elucidated, PBF is implicated in cell transformation, migration and invasion (13, 22, 30). We thus propose that PBF should be considered a novel prognostic marker of poor outcome in HNSCC.

p53 is frequently mutated in HNSCC (7, 36, 42) or is inactivated by other mechanisms, including HPV E6 oncoprotein expression (10), thus supporting the importance of loss or gain of p53 function to promote HNSCC tumour initiation and progression. Given that PTTG and PBF are known to modulate p53 activity in several tumour settings (11–13) and that they were both induced in our series of HNSCC, we further investigated their precise relationship and roles in tumorigenesis.

An important relationship was highlighted by extensive correlation between PTTG and p53-target genes in wild-type p53 tumours in TCGA. Our experiments in HNSCC cells *in vitro* indicated a causal link for this association as PTTG bound and decreased p53 stability, as well as providing supportive evidence of altered expression of key p53-target genes such as

BCL2 following ablation of PTTG. A reduced correlation between PTTG and p53-target genes would be expected in mutant p53 tumours as TP53 gene alterations affect p53 transcriptional activity by disrupting DNA contact or protein conformation (43). In agreement with this, a significant reduction in correlated genes was observed but, interestingly, there was still nearly 58% of p53-target genes correlated with PTTG expression in mutant p53 tumours. Exogenous PBF also bound and decreased p53 stability in HNSCC cells *in vitro*. However, in contrast to PTTG, there were fewer p53-target genes correlated with PBF expression in wild-type or mutant p53 tumours. Considering the heterogeneity of HNSCC, our findings suggest that extensive correlation between PBF and p53-target genes might instead occur in particular HNSCC subgroups. We observed, for instance, greater correlation of PBF with p53-target genes (up to 50%) in HNSCC tumours with both high PBF and PTTG expression.

The precise relationship of PBF and PTTG with mutant p53 protein requires further study especially as we have reported that PBF binds to p53 mutants such as R273C in colorectal tumours, which are also common in HNSCC (13, 36). It is unlikely that PBF diminishes the stability of mutant p53 as high PBF levels did not destabilise mutant p53 protein in colorectal tumours (13). Instead, PBF might be similar to Sp1 and other factors that cooperate with mutant p53 to enhance or repress target gene expression (44). Gene correlations in mutant p53 HNSCC with PBF or PTTG might therefore be a consequence of functional interactions with mutant p53 proteins that have retained transcriptional activity (44), as well as with wild-type p53 that is present and co-exists with mutant p53 protein, especially at earlier stages of tumour evolution (36). We will also need to investigate whether PTTG and PBF can regulate p53-target genes via pathways independent of p53 function.

Five-year survival rates of HNSCC patients range from 27 up to 71% depending on tumour aggressiveness and subsite location (45). In agreement with previous studies, we found that HNSCC patients with mutant p53 had worse survival characteristics than those with wild-type p53 (36). Of particular significance, in the current study we further demonstrate that PTTG and PBF together, as well as TP53 alterations, should be considered as an important clinical indicator of tumour behaviour in HNSCC, particularly for more aggressive malignancies. These results will facilitate the identification and earlier treatment of more aggressive forms of HNSCC. Importantly, monitoring PBF expression was also a useful prognostic marker for HNSCC tumours with wild-type p53, as well as mutant p53. The findings from this and other studies (22, 30, 31, 46–48) indicate that PTTG and PBF have a multitude of roles in different tumour types such as breast, colorectal and ovarian. It will be important to determine whether PTTG and PBF have additional oncogenic roles in HNSCC, apart from their impact on p53-target genes and cellular invasion, especially as both proteins were overexpressed in oropharyngeal tumours of all stages. In particular, the recapitulation of our findings in a suitable animal model of HNSCC could facilitate future insights into the oncogenic roles of PBF and PTTG (49).

Interestingly, we found that joint over-expression of PTTG and PBF apparent in HNSCC tumours appeared to markedly decrease p53 stability *in vitro*. Thus, p53 stability was lowest when both PTTG and PBF were overexpressed. To tease apart the relative contributions of

each gene, we employed mutants which prevented their interaction. For instance, p53 stability was not altered by PBF M1 mutant, which retains p53 interaction (13) but lacks the C-terminal 30 amino acids that mediate binding to PTTG (38); thus implying that recruitment of PTTG to p53 by PBF is mandatory to effectively inhibit p53. In contrast, p53 turnover was still increased by PBF when co-expressed with the PTTG BD- mutant although by a lesser extent than with WT PTTG. PBF therefore appears capable of targeting p53 for MDM2-mediated ubiquitination (12) even with weaker recruitment of PTTG (38). The binding interaction between PTTG and p53 was significantly repressed in PBF-depleted HNSCC cells, thus further supporting that PBF facilitates PTTG:p53 binding. Conversely, PBF bound p53 more readily when PTTG was ablated; one possibility being that without competition to bind PTTG, more 'free' PBF is available to bind p53. Interestingly, the binding sites for PTTG and PBF appear to be located within overlapping regions of the p53 protein (PTTG: amino acids 300-374 (11); PBF: amino acids 318-393 (12)). Based on these observations we therefore propose that PBF recruits PTTG to the same region of p53.

In summary, we show for the first time that the proto-oncogene PBF interacts with its binding partner PTTG to inhibit p53 stability - a key tumour suppressor protein. Together with its fundamental role in cellular invasion, this study demonstrates that PBF is of critical relevance to head and neck cancer. Hence, HNSCC patients with high tumoural PBF and PTTG have worse outcomes due in part to greater aberration of p53-dependent signalling.

## Supplementary Material

Refer to Web version on PubMed Central for supplementary material.

## Acknowledgments

Results are in part based upon data generated by the TCGA Research Network: <http://cancergenome.nih.gov/>. We acknowledge the following funding sources: Medical Research Council (grant number MR/P000509/1; to C.J. McCabe, V.E. Smith and K. Boelaert) and the Wellcome Trust (to C.J. McCabe and H. Mehanna).

## References

1. Ferlay J, Soerjomataram I, Dikshit R, Eser S, Mathers C, Rebelo M, et al. Cancer incidence and mortality worldwide: sources, methods and major patterns in GLOBOCAN 2012. *Int J Cancer*. 2015; 136:E359–86. [PubMed: 25220842]
2. Global Burden of Disease Cancer C, Fitzmaurice C, Allen C, Barber RM, Barregard L, Bhutta ZA, et al. Global, Regional, and National Cancer Incidence, Mortality, Years of Life Lost, Years Lived With Disability, and Disability-Adjusted Life-years for 32 Cancer Groups, 1990 to 2015: A Systematic Analysis for the Global Burden of Disease Study. *JAMA Oncol*. 2017; 3:524–48. [PubMed: 27918777]
3. Chung CH, Parker JS, Karaca G, Wu J, Funkhouser WK, Moore D, et al. Molecular classification of head and neck squamous cell carcinomas using patterns of gene expression. *Cancer Cell*. 2004; 5:489–500. [PubMed: 15144956]
4. Rampias T, Pectasides E, Prasad M, Sasaki C, Gouveris P, Dimou A, et al. Molecular profile of head and neck squamous cell carcinomas bearing p16 high phenotype. *Ann Oncol*. 2013; 24:2124–31. [PubMed: 23406730]
5. Walter V, Yin X, Wilkerson MD, Cabanski CR, Zhao N, Du Y, et al. Molecular subtypes in head and neck cancer exhibit distinct patterns of chromosomal gain and loss of canonical cancer genes. *PLoS One*. 2013; 8:e56823. [PubMed: 23451093]

6. Keck MK, Zuo Z, Khattri A, Stricker TP, Brown CD, Imanguli M, et al. Integrative analysis of head and neck cancer identifies two biologically distinct HPV and three non-HPV subtypes. *Clin Cancer Res.* 2015; 21:870–81. [PubMed: 25492084]
7. Cancer Genome Atlas N. Comprehensive genomic characterization of head and neck squamous cell carcinomas. *Nature.* 2015; 517:576–82. [PubMed: 25631445]
8. Agrawal N, Frederick MJ, Pickering CR, Bettegowda C, Chang K, Li RJ, et al. Exome sequencing of head and neck squamous cell carcinoma reveals inactivating mutations in NOTCH1. *Science.* 2011; 333:1154–7. [PubMed: 21798897]
9. Stransky N, Egloff AM, Tward AD, Kostic AD, Cibulskis K, Sivachenko A, et al. The mutational landscape of head and neck squamous cell carcinoma. *Science.* 2011; 333:1157–60. [PubMed: 21798893]
10. Scheffner M, Werness BA, Huibregtse JM, Levine AJ, Howley PM. The E6 oncoprotein encoded by human papillomavirus types 16 and 18 promotes the degradation of p53. *Cell.* 1990; 63:1129–36. [PubMed: 2175676]
11. Bernal JA, Luna R, Espina A, Lazaro I, Ramos-Morales F, Romero F, et al. Human securin interacts with p53 and modulates p53-mediated transcriptional activity and apoptosis. *Nat Genet.* 2002; 32:306–11. [PubMed: 12355087]
12. Read ML, Seed RI, Fong JC, Modasia B, Ryan GA, Watkins RJ, et al. The PTTG1-binding factor (PBF/PTTG1IP) regulates p53 activity in thyroid cells. *Endocrinology.* 2014; 155:1222–34. [PubMed: 24506068]
13. Read ML, Seed RI, Modasia B, Kwan PP, Sharma N, Smith VE, et al. The proto-oncogene PBF binds p53 and is associated with prognostic features in colorectal cancer. *Mol Carcinog.* 2016; 55:15–26. [PubMed: 25408419]
14. Shibata Y, Haruki N, Kuwabara Y, Nishiwaki T, Kato J, Shinoda N, et al. Expression of PTTG (pituitary tumor transforming gene) in esophageal cancer. *Jpn J Clin Oncol.* 2002; 32:233–7. [PubMed: 12324572]
15. Zhou C, Liu S, Zhou X, Xue L, Quan L, Lu N, et al. Overexpression of human pituitary tumor transforming gene (hPTTG), is regulated by beta-catenin /TCF pathway in human esophageal squamous cell carcinoma. *Int J Cancer.* 2005; 113:891–8. [PubMed: 15514942]
16. Ito T, Shimada Y, Kan T, David S, Cheng Y, Mori Y, et al. Pituitary tumor-transforming 1 increases cell motility and promotes lymph node metastasis in esophageal squamous cell carcinoma. *Cancer Res.* 2008; 68:3214–24. [PubMed: 18451147]
17. Yan S, Zhou C, Lou X, Xiao Z, Zhu H, Wang Q, et al. PTTG overexpression promotes lymph node metastasis in human esophageal squamous cell carcinoma. *Cancer Res.* 2009; 69:3283–90. [PubMed: 19351864]
18. Zhang J, Yang Y, Chen L, Zheng D, Ma J. Overexpression of pituitary tumor transforming gene (PTTG) is associated with tumor progression and poor prognosis in patients with esophageal squamous cell carcinoma. *Acta Histochem.* 2014; 116:435–9. [PubMed: 24176776]
19. Zhou C, Liu S, Zhou X, Xue L, Quan L, Lu N, et al. Overexpression of human pituitary tumor transforming gene (hPTTG), is regulated by beta-catenin /TCF pathway in human esophageal squamous cell carcinoma. *Int J Cancer.* 2005; 113:891–8. [PubMed: 15514942]
20. Read ML, Fong JC, Modasia B, Fletcher A, Imruetaicharoenchoke W, Thompson RJ, et al. Elevated PTTG and PBF predicts poor patient outcome and modulates DNA damage response genes in thyroid cancer. *Oncogene.* 2017; 36:5296–308. [PubMed: 28504713]
21. Cancer Genome Atlas Research N. Integrated genomic characterization of papillary thyroid carcinoma. *Cell.* 2014; 159:676–90. [PubMed: 25417114]
22. Stratford AL, Boelaert K, Tannahill LA, Kim DS, Warfield A, Eggo MC, et al. Pituitary tumor transforming gene binding factor: a novel transforming gene in thyroid tumorigenesis. *J Clin Endocrinol Metab.* 2005; 90:4341–9. [PubMed: 15886233]
23. Watkins RJ, Read ML, Smith VE, Sharma N, Reynolds GM, Buckley L, et al. Pituitary Tumor Transforming Gene Binding Factor: a New Gene in Breast Cancer. *Cancer Res.* 2010; 70:3739–49. [PubMed: 20406982]



24. Smith VE, Read ML, Turnell AS, Watkins RJ, Watkinson JC, lewy gd, et al. A novel mechanism of sodium iodide symporter repression in differentiated thyroid cancer. *J Cell Sci.* 2009; 122:3393–402. [PubMed: 19706688]
25. Cerami E, Gao J, Dogrusoz U, Gross BE, Sumer SO, Aksoy BA, et al. The cBio cancer genomics portal: an open platform for exploring multidimensional cancer genomics data. *Cancer Discov.* 2012; 2:401–4. [PubMed: 22588877]
26. Gao J, Aksoy BA, Dogrusoz U, Dresdner G, Gross B, Sumer SO, et al. Integrative analysis of complex cancer genomics and clinical profiles using the cBioPortal. *Sci Signal.* 2013; 6:p11. [PubMed: 23550210]
27. Broad Institute TCGA Genome Data Analysis Center. Broad Institute of MIT and Harvard; 2016. Analysis-ready standardized TCGA data from Broad GDAC Firehose 2016\_01\_28 run. Dataset.
28. Mora-Santos M, Castilla C, Herrero-Ruiz J, Giraldez S, Limon-Mortes MC, Saez C, et al. A single mutation in Securin induces chromosomal instability and enhances cell invasion. *Eur J Cancer.* 2013; 49:500–10. [PubMed: 22819078]
29. Smith VE, Sharma N, Watkins RJ, Read ML, Ryan GA, Kwan PP, et al. Manipulation of PBF/PTTG1IP phosphorylation status; a potential new therapeutic strategy for improving radioiodine uptake in thyroid and other tumors. *J Clin Endocrinol Metab.* 2013; 98:2876–86. [PubMed: 23678037]
30. Watkins RJ, Imruetaicharoenchoke W, Read ML, Sharma N, Poole VL, Gentilin E, et al. Pro-invasive Effect of Proto-oncogene PBF Is Modulated by an Interaction with Cortactin. *J Clin Endocrinol Metab.* 2016; 101:4551–63. [PubMed: 27603901]
31. Yoon CH, Kim MJ, Lee H, Kim RK, Lim EJ, Yoo KC, et al. PTTG1 oncogene promotes tumor malignancy via epithelial to mesenchymal transition and expansion of cancer stem cell population. *J Biol Chem.* 2012; 287:19516–27. [PubMed: 22511756]
32. Lin YH, Tian Y, Wang JS, Jiang YG, Luo Y, Chen YT. Pituitary tumor-transforming gene 1 regulates invasion of prostate cancer cells through MMP13. *Tumour Biol.* 2015; 37:15495–500.
33. Rubinek T, Chesnokova V, Wolf I, Wawrowsky K, Vlotides G, Melmed S. Discordant proliferation and differentiation in pituitary tumor-transforming gene-null bone marrow stem cells. *Am J Physiol Cell Physiol.* 2007; 293:C1082–C92. [PubMed: 17626243]
34. Chesnokova V, Wong C, Zonis S, Gruszka A, Wawrowsky K, Ren SG, et al. Diminished pancreatic beta-cell mass in securin-null mice is caused by beta-cell apoptosis and senescence. *Endocrinology.* 2009; 150:2603–10. [PubMed: 19213844]
35. Hsu YH, Liao LJ, Yu CH, Chiang CP, Jhan JR, Chang LC, et al. Overexpression of the pituitary tumor transforming gene induces p53-dependent senescence through activating DNA damage response pathway in normal human fibroblasts. *J Biol Chem.* 2010; 285:22630–8. [PubMed: 20452981]
36. Zhou G, Liu Z, Myers JN. TP53 Mutations in Head and Neck Squamous Cell Carcinoma and Their Impact on Disease Progression and Treatment Response. *J Cell Biochem.* 2016; 117:2682–92. [PubMed: 27166782]
37. Salehi F, Kovacs K, Scheithauer BW, Lloyd RV, Cusimano M. Pituitary tumor-transforming gene in endocrine and other neoplasms: a review and update. *Endocr Relat Cancer.* 2008; 15:721–43. [PubMed: 18753362]
38. Chien W, Pei L. A novel binding factor facilitates nuclear translocation and transcriptional activation function of the pituitary tumor-transforming gene product. *J Biol Chem.* 2000; 275:19422–7. [PubMed: 10781616]
39. Beck TN, Golemis EA. Genomic insights into head and neck cancer. *Cancers Head Neck.* 2016; 1doi: 10.1186/s41199-016-0003-z
40. Heaney AP, Horwitz GA, Wang Z, Singson R, Melmed S. Early involvement of estrogen-induced pituitary tumor transforming gene and fibroblast growth factor expression in prolactinoma pathogenesis. *Nat Med.* 1999; 5:1317–21. [PubMed: 10546001]
41. Xiang C, Gao H, Meng L, Qin Z, Ma R, Liu Y, et al. Functional variable number of tandem repeats variation in the promoter of proto-oncogene PTTG1IP is associated with risk of estrogen receptor-positive breast cancer. *Cancer Sci.* 2012; 103:1121–8. [PubMed: 22404099]



42. Petitjean A, Achatz MI, Borresen-Dale AL, Hainaut P, Olivier M. TP53 mutations in human cancers: functional selection and impact on cancer prognosis and outcomes. *Oncogene*. 2007; 26:2157–65. [PubMed: 17401424]
43. Bullock AN, Fersht AR. Rescuing the function of mutant p53. *Nat Rev Cancer*. 2001; 1:68–76. [PubMed: 11900253]
44. Freed-Pastor WA, Prives C. Mutant p53: one name, many proteins. *Genes Dev*. 2012; 26:1268–86. [PubMed: 22713868]
45. Braakhuis BJ, Leemans CR, Visser O. Incidence and survival trends of head and neck squamous cell carcinoma in the Netherlands between 1989 and 2011. *Oral Oncol*. 2014; 50:670–5. [PubMed: 24735546]
46. Wang X, Duan W, Li X, Liu J, Li D, Ye L, et al. PTTG regulates the metabolic switch of ovarian cancer cells via the c-myc pathway. *Oncotarget*. 2015; 6:40959–69. [PubMed: 26516926]
47. Zheng Y, Guo J, Zhou J, Lu J, Chen Q, Zhang C, et al. FoxM1 transactivates PTTG1 and promotes colorectal cancer cell migration and invasion. *BMC Med Genomics*. 2015; 8:49. [PubMed: 26264222]
48. Gao H, Zhong F, Xie J, Peng J, Han Z. PTTG promotes invasion in human breast cancer cell line by upregulating EMMPRIN via FAK/Akt/mTOR signaling. *Am J Cancer Res*. 2016; 6:425–39. [PubMed: 27186413]
49. Supravhad W, Dirksen WP, Martin CK, Rosol TJ. Animal models of head and neck squamous cell carcinoma. *Vet J*. 2016; 210:7–16. [PubMed: 26965084]

### **Significance**

Findings reveal a complex and novel interrelationship between the expression and function of PTTG, PBF, and p53 in human HNSCC that significantly influences patient outcome.

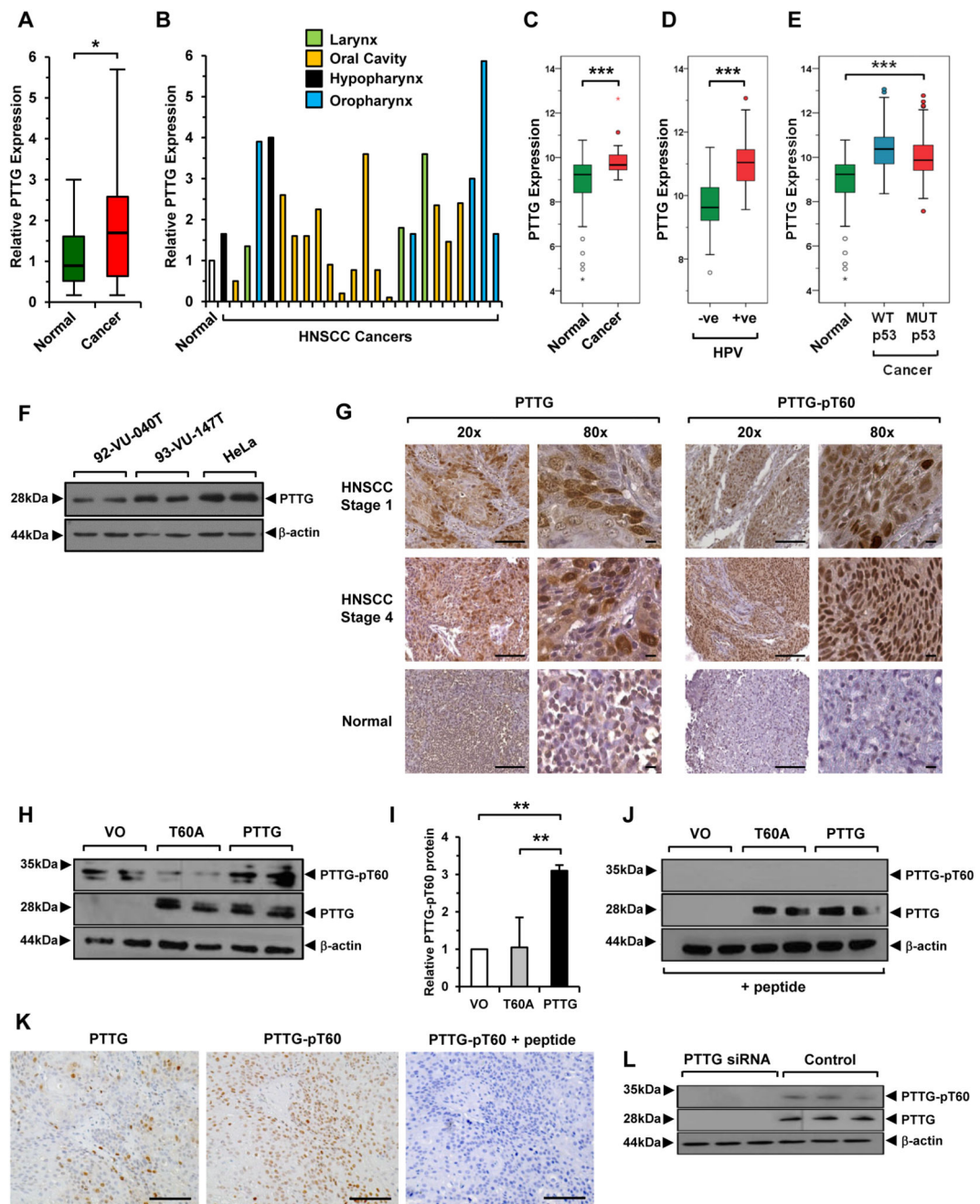


**Figure 1. Increased PTTG expression and phosphorylation.**

**A**, PTTG mRNA expression in HNSCC (cancer) relative to matched normal; \*,  $P < 0.05$ . **B**, Individual PTTG mRNA levels at HNSCC subsites. **C-E**, Box-whisker plots of PTTG expression in **(C)** matched (normal/cancer) TCGA data, **(D)** HPV (-ve) versus (+ve) HNSCC and **(E)** unmatched HNSCC with either WT or MUT p53 relative to normal; \*\*\* $P < 0.001$ . **F**, Western blot analysis of PTTG expression in HNSCC cell lines used in study compared to HeLa cells. **G**, Representative images of PTTG (total and pT60) in HNSCC/normal tissue. Images at 20x (scale bars, 100 $\mu$ m) and 80x (scale bars, 10 $\mu$ m) magnification. **H**, Western

blot analysis of PTTG (total and pT60) in HeLa cells transfected with WT PTTG, T60A mutant or vector only (VO). **I**, Quantification of PTTG-pT60 from (**H**); \*\* $P < 0.01$ . **J**, Same as (**H**) but Western blot preincubated with neutralising peptide. **K**, Same as (**G**) but HNSCC tissue preincubated with neutralising peptide prior to immunostaining. (right) Control images of PTTG (left) and PTTG-pT60 (middle) in HNSCC tissue without neutralising peptide. Scale bars, 100  $\mu\text{m}$ . **L**, Western blot analysis of PTTG (total and pT60) in HeLa cells transfected with PTTG or control siRNA.

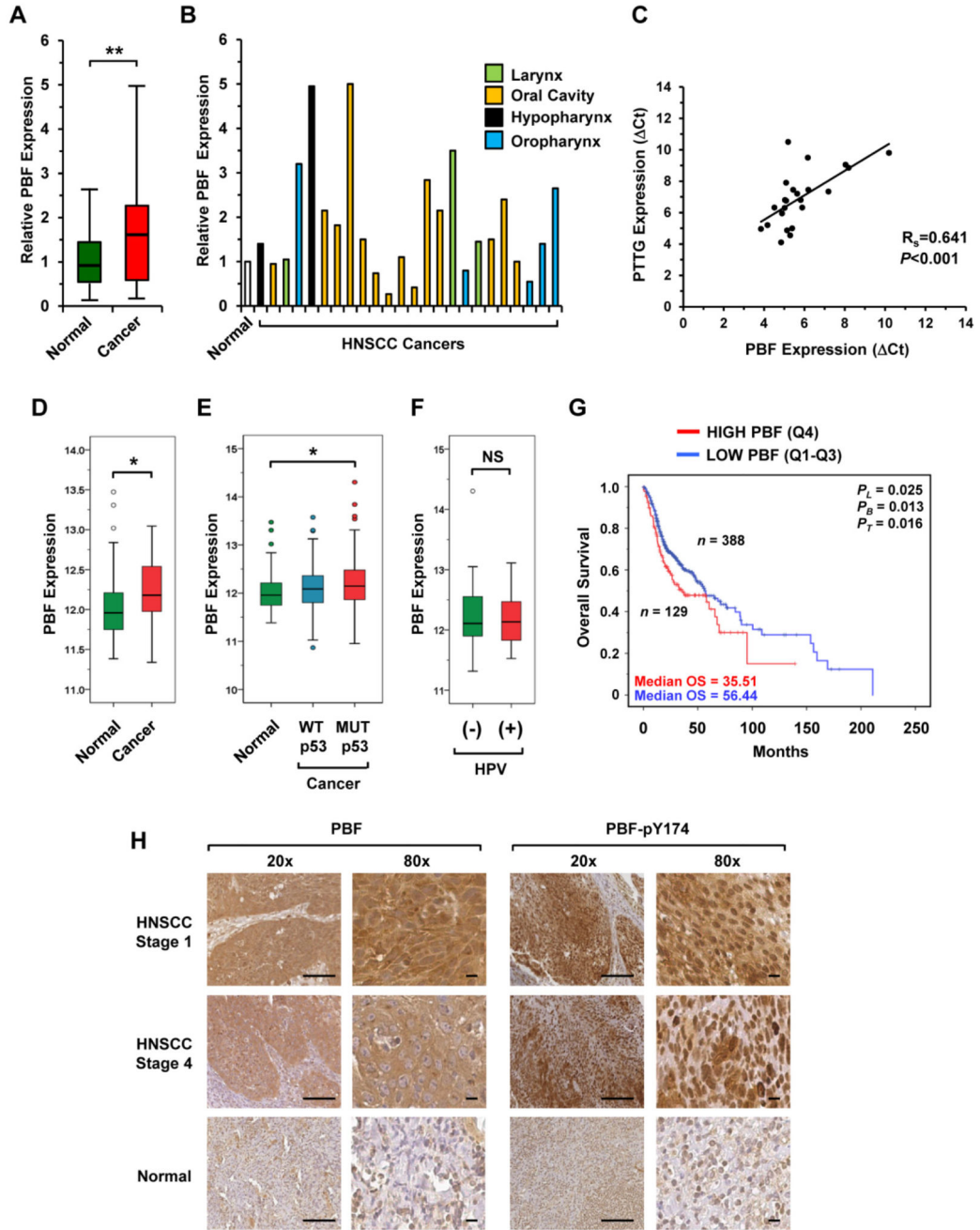


**Figure 2. Elevated PBF expression and poorer survival.**

**A**, PBF mRNA expression in HNSCC (cancer) relative to matched normal;  $**P < 0.01$ . **B**, Individual PBF mRNA levels at HNSCC subsites. **C**, Correlation of PBF and PTTG mRNA expression in HNSCC;  $***P < 0.001$ . **D-F**, Box-whisker plots showing PBF expression in **(D)** matched (normal/cancer) TCGA data, **(E)** unmatched HNSCC with either WT or MUT p53 relative to normal, and **(F)** HPV (-ve) versus (+ve) HNSCC; NS, not-significant;  $*P < 0.05$ . **G**, Overall survival for HNSCC with high (top 25 percentile) versus low tumoural PBF expression (bottom 75 percentile) in TCGA;  $*P < 0.05$ . **H**, Representative images of PBF

(total and pY174) in HNSCC and normal tissue. Images at 20x (scale bars, 100 $\mu$ m) and 80x (scale bars, 10 $\mu$ m) magnification.



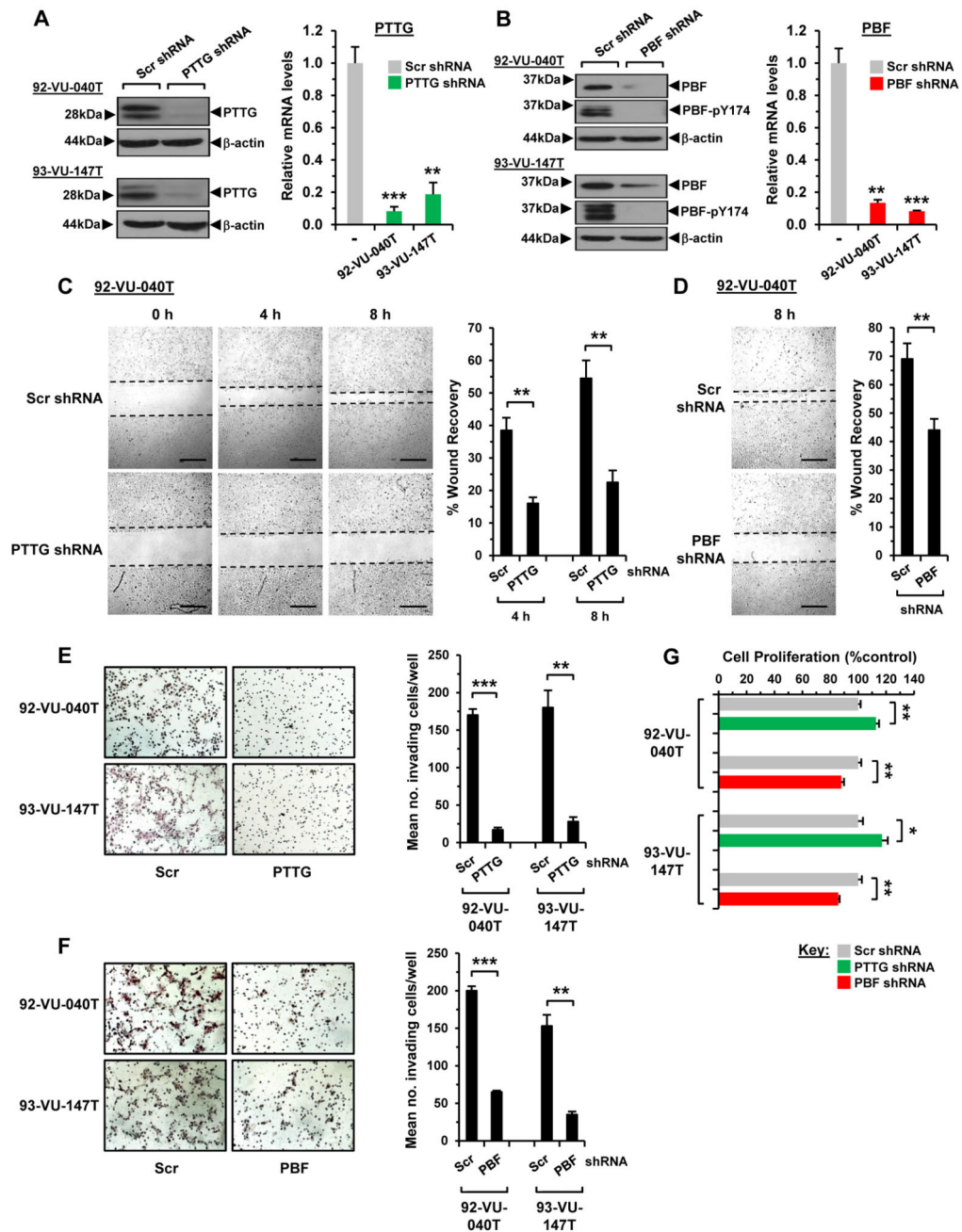


**Figure 3. Depletion of PTTG and PBF abrogates cell movement.**

**A**, Relative PTTG protein (left) and mRNA expression (right) in HNSCC cells transduced with PTTG or Scr shRNA; \*\* $P < 0.01$ ; \*\*\* $P < 0.001$ . **B**, Same as (A) but relative PBF expression in PBF shRNA transduced cells. **C**, Representative images of scratch wound assays in 92-VU-040T cells transduced with PTTG or Scr shRNA. Images taken after 0, 4 and 8h. Scale bars, 500 $\mu$ m. (right) % wound recovery at indicated time points; \*\* $P < 0.01$ . **D**, Same as (C) but wound healing in PBF shRNA transduced cells. **E**, Representative photomicrographs of 2D Boyden cell invasion assays in HNSCC cells transduced with

PTTG or Scr shRNA. (right) Quantification of invading cells; \*\* $P < 0.01$ ; \*\*\* $P < 0.001$ . **F**, Same as (**E**) but cells transduced with PBF shRNA. **G**, Proliferation of HNSCC cells transduced with PTTG, PBF or Scr shRNA; \* $P < 0.05$ ; \*\* $P < 0.01$ . Data presented as mean  $\pm$ SE.

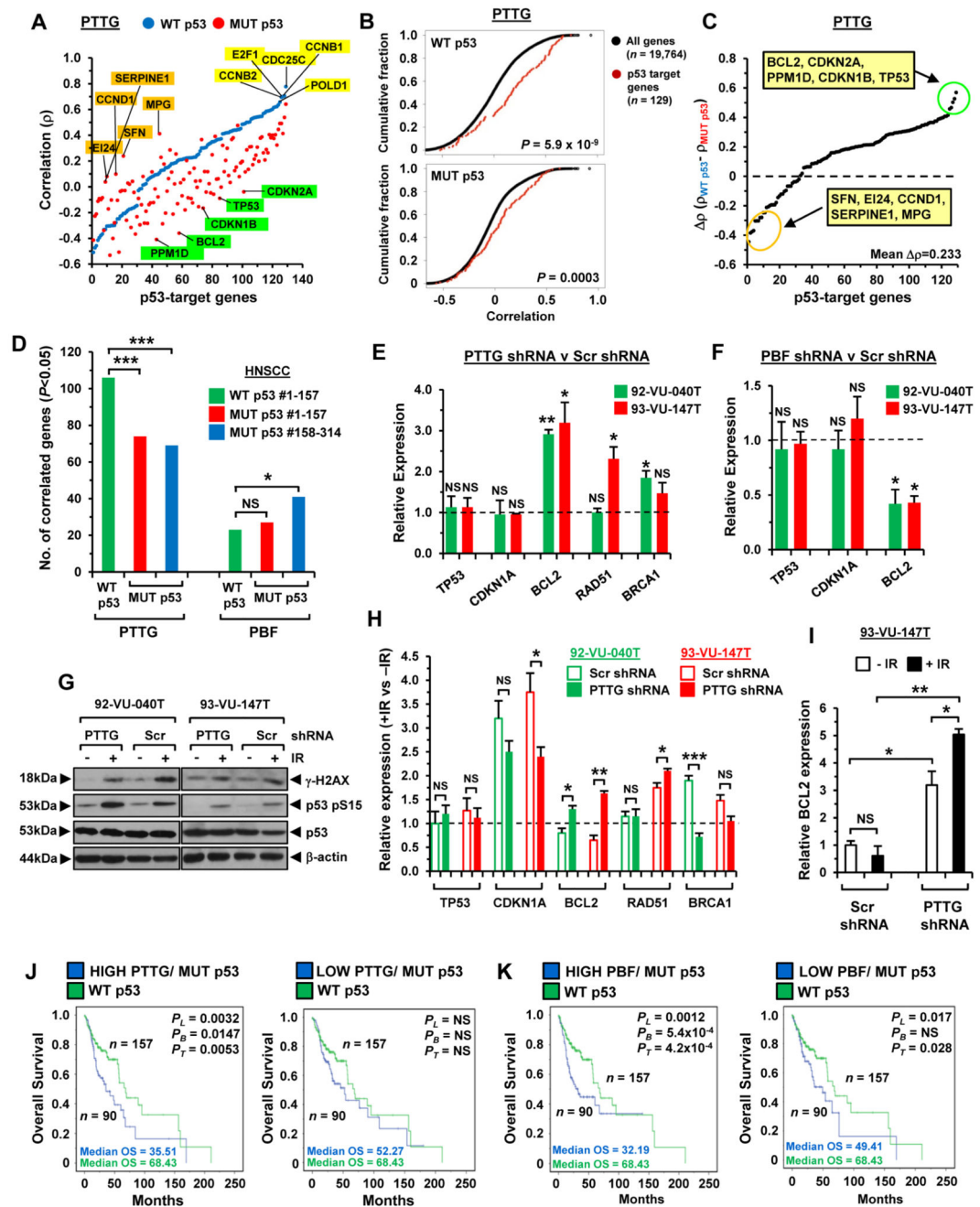


**Figure 4. Association of PTTG and PBF with p53-target genes.**

**A**, Correlation pattern of PTTG with 129 p53-target genes in unmatched HNSCC with WT p53 (blue dots) and MUT p53 (red dots). **B**, Cumulative distribution plot comparing the correlations between PTTG with all detectable genes versus p53-target genes in WT (upper) and MUT p53 (lower) HNSCC. **C**, Differences in  $\rho$  values for p53-target genes between WT and MUT p53 HNSCC. **D**, p53-target genes significantly correlated with PTTG or PBF in WT and MUT p53 HNSCC ( $n=157$  per cohort; NS, not significant; \* $P<0.05$ ; \*\*\* $P<0.001$ ). **E**, Relative mRNA expression of indicated genes in PTTG or Scr shRNA transduced cells.

Data presented as mean±SE. **F**, Same as (**E**) but cells transduced with PBF shRNA. **G**, Western blot analysis of  $\gamma$ -H2AX, p53 S15 and p53 in PTTG or Scr shRNA transduced cells irradiated with 15-Gy dose. **H**, Relative fold-change in mRNA expression of indicated genes following irradiation (+IR) of PTTG or Scr shRNA transduced cells versus non-irradiated controls (-IR). (NS, not significant; \* $P<0.05$ ; \*\* $P<0.01$ ; \*\*\* $P<0.001$ ). **I**, BCL2 expression relative to levels in Scr shRNA transduced cells (-IR). **J**, Overall survival for MUT p53 HNSCC with high (Q4, left) or low (Q1, right) PTTG expression compared to WT p53 HNSCC. **K**, Overall survival for MUT p53 HNSCC with high (Q4, left) or low (Q1, right) PBF expression compared to WT p53 HNSCC.

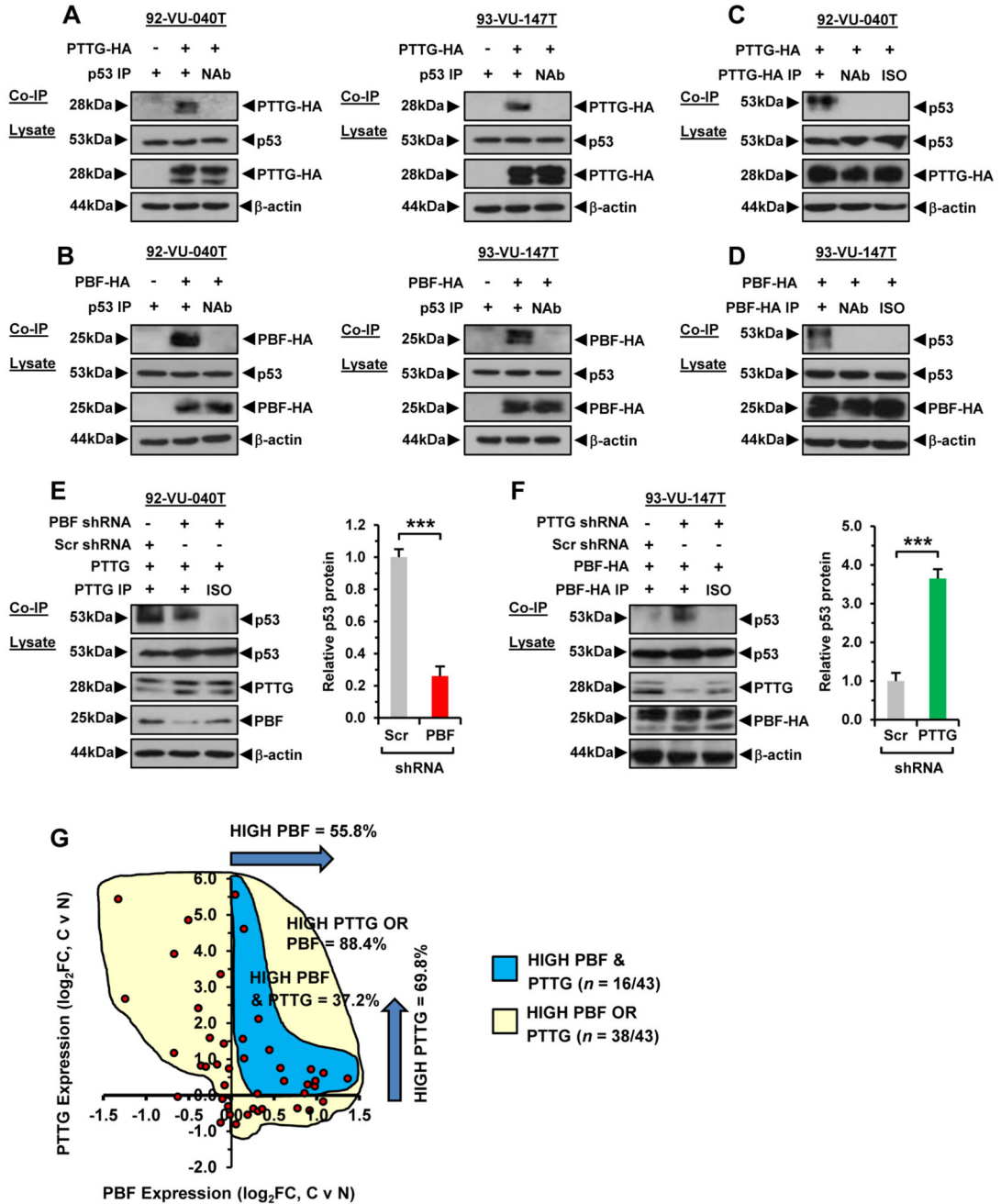


**Figure 5. PTTG and PBF reciprocally alter stringency of binding to p53.**  
**A**, Co-IP assays in 92-VU-040T (left) and 93-VU-147T cells (right) showing specific interaction between PTTG-HA and p53. **B**, Same as **(A)** but specific interaction between PBF-HA and p53. **C**, Reciprocal co-IP assay in 92-VU-040T cells showing specific interaction between PTTG-HA and p53. **D**, Same as **(C)** but specific interaction between PBF-HA and p53 in 93-VU-147T cells. **E**, Co-IP assay in PBF shRNA transduced 92-VU-040T cells showing reduced interaction between PTTG and p53. (right) Mean p53 protein levels relative to β-actin. Data presented as mean±SE; \*\*\**P*<0.001. **F**, Co-IP assay in

PTTG shRNA transduced 93-VU-147T cells showing greater interaction between PBF and p53. (right) Mean p53 protein levels relative to  $\beta$ -actin. Data presented as mean $\pm$ SE; \*\*\* $P$ <0.001. **G**, Scatterplot showing fold change (FC) in PBF and PTTG expression in HNSCC versus matched normal samples ( $\log_2$ ,  $n = 43$ , TCGA data set).



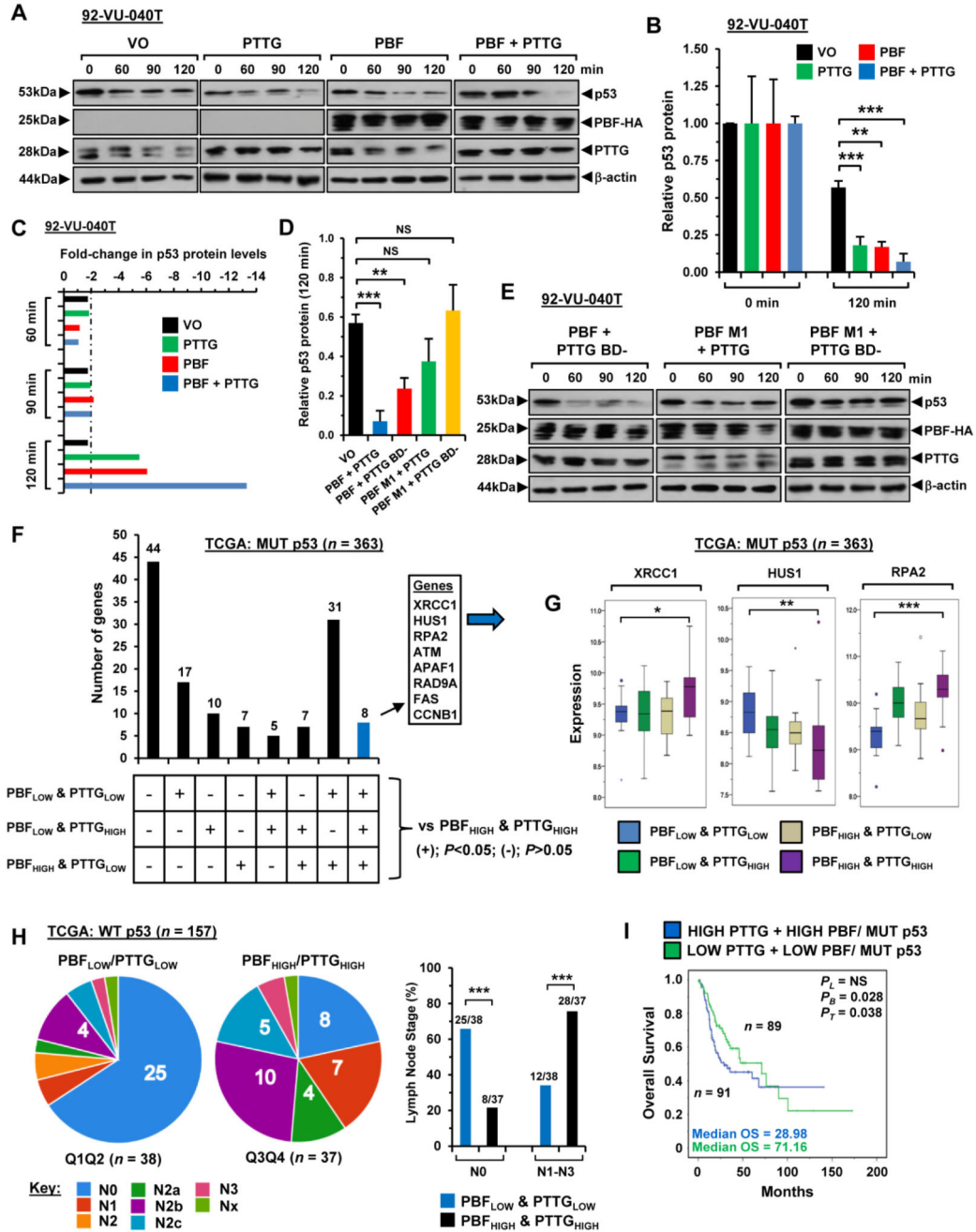


**Figure 6. Impact of PBF and PTTG on dynamics of p53 turnover.**

**A**, Western Blot analysis of p53 stability in 92-VU-040T cells transfected with VO, PBF, PTTG or PBF+PTTG and lysed at indicated times post-treatment with anisomycin. **B**, Mean p53 protein levels normalised to β-actin from half-life study described in (A). Data presented as mean±SE from 3 independent experiments; \*\*P<0.001; \*\*\*P<0.001. **C**, Fold-changes in relative p53 protein levels normalised to β-actin at indicated time points post-anisomycin treatment in 92-VU-040T cells. **D-E**, p53 stability assays as in (A) and (B) but using 92-VU-040T cells transfected with PBF M1+PTTG, PBF+PTTG BD- or PBF

M1+BD-. **F**, Differentially expressed p53-target genes in MUT p53 HNSCC with high PBF/PTTG expression versus other PBF/PTTG expression subgroups. **G**, Box whisker plots for XRCC1, HUS1 and RPA2 in PBF/PTTG expression subgroups in MUT p53 HNSCC as identified in (F); \* $P < 0.05$ ; \*\* $P < 0.001$ ; \*\*\* $P < 0.001$ . **H**, Association of PBF/PTTG expression subgroups with lymph node staging in WT p53 HNSCC; \*\*\* $P < 0.001$ ; Fisher's exact test. **I**, Overall survival for MUT p53 HNSCC with high versus low PBF/PTTG expression. Median PBF and PTTG expression values used to stratify patients into subgroups.

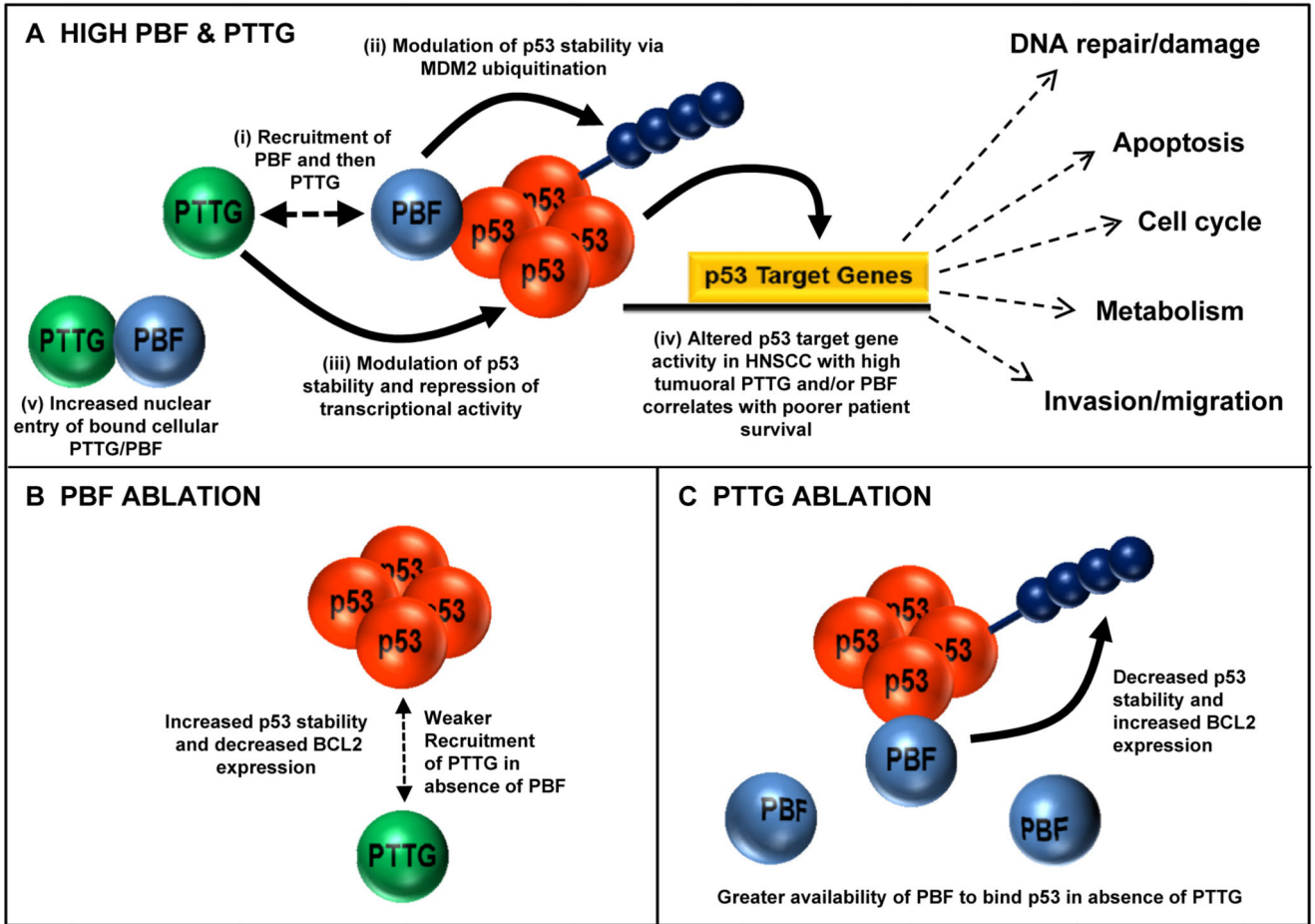


**Figure 7. Proposed model of PTTG, PBF and p53 functional interaction.**

**A**, (i) PBF binds p53 and recruits PTTG. (ii) PBF targets p53 ubiquitination via MDM2 while (iii) PTTG can modulate p53 stability and repress transcriptional activity. (iv) PTTG and PBF cooperate to disrupt p53 pathways associated with processes such as DNA damage repair to promote tumorigenesis. High PTTG and/or PBF correlates with poorer HNSCC patient survival. (v) High tumoural PBF expression also promotes nuclear uptake of PTTG. **B**, PBF ablation weakens recruitment of PTTG to p53 thereby reducing capacity to modulate p53 stability. **C**, PTTG ablation increases PBF availability to bind p53 due to diminished PBF:PTTG interaction.